Chirality

Deutsche Ausgabe: DOI: 10.1002/ange.201510123
Internationale Ausgabe: DOI: 10.1002/anie.201510123

# Monolayer Filaments versus Multilayer Stacking of Bent-Core Molecules

*Joanna Matraszek, Neha Topnani, Natasa Vaupotič, Hideo Takezoe, Jozef Mieczkowski, Damian Pociecha, and Ewa Gorecka**

***Abstract:*** *Bent-core materials exhibiting lamellar crystals (B4 phase), when dissolved in organic solvents, formed gels with helical ribbons made of molecular monolayers and bilayers, whereas strongly deformed stacks of 5–6 layers were found in the bulk samples. The width and pitch of the helical filaments were governed by molecular length; they both increased with terminal-chain elongation. It was also found that bulk samples were optically active, in contrast to the corresponding gels, which lacked optical activity. The optical activity of samples originated from the internal structure of the crystal layers rather than from the helicity of the filaments. A theoretical model predicts a strong increase in optical activity as the number of layers in the stack increases and its saturation for few layers, thus explaining the smaller optical activity for gels than for bulk samples. A strong increase and redshift in fluorescence was detected in gels as compared to the sol state.*

Organogels of small molecules have attracted much attention[1] owing to their complex morphology[2] and functions.[3] Another interesting topic is the chirality of self-assembled fibrils that form gels,[4] in which rods, tapes, or tubes may be helically twisted, coiled, or wound, and the length, diameter, and chiral pitch of the fibers are highly variable: from approximately 10 nm to 1 mm. The chirality expressed at the nano- and microscales might result from the molecular chirality,[5] but also achiral molecules can form helical superstructures, for example, through hydrogen bonding[6] or the existence of conformational chirality.[7]

Herein we focus on achiral bent-core mesogens, which are able to form hierarchical chiral structures. Among them, the B4 phase is particularly intriguing. This lamellar crystalline phase is assumed to have a morphology consisting of helical twisted ribbons built of just a few molecular layers. The chiral symmetry breaking that occurs in the B4 phase at the microscale results in the formation of large homochiral optically active (OA) areas. Recently, excellent gelation ability was reported for B4 materials made of rigid bent-core molecules[8] and flexible dimers.[9] Mixtures of compounds exhibiting the B4 phase and organic materials are phase-segregated; therefore, helical nanofilaments can be expected to remain in the gel in their original morphology.[10]

In this study, to correlate gelation ability with the crystalline structure of filaments, we investigated a bent-core molecular system that exhibits the metastable B4 phase upon rapid cooling from the isotropic liquid. The morphology of the B4 phase was found to be different for bulk and gel samples, despite the same crystallographic structure. The optical activity of the B4 phase is discussed in relation to the morphology of the samples.

A series of bent-core molecules with the same mesogenic core and a variety of end chains, including chiral end chains, was synthesized (see the Supporting Information). The studied compounds are new, although molecules with the same bent mesogenic core have been already reported, with unsaturated terminal chains[11] or bulky substituents at the central ring.[12] The chemical structures and the phase sequences are summarized in Table 1. On cooling from the isotropic liquid, compound **11**, with a nitro group at the central ring, showed characteristic textures with spiraling features suggesting the B7 phase.[13] X-ray crystallographic studies revealed a structure made of smectic layer fragments arranged in a 2D oblique lattice[14] with a primitive crystallographic unit cell: $a = 8.60$ nm, $b = 3.73$ nm, and $\gamma = 109.2°$ at 120 °C (see the Supporting Information). The other studied materials exhibited no liquid-crystalline phases but a complicated polymorphism of crystal types depending on the cooling rate. The crystals obtained by slow cooling ($< 10\,°C\,min^{-1}$) were birefringent and optically inactive. However, if the samples with linear *n*-alkyl tails (compounds **2**–**5**) were rapidly cooled ($> 20\,°C\,min^{-1}$) from the isotropic melt, textures characteristic of the B4 phase, with large domains that were not or were only weakly birefringent and optically active (optical rotatory power, $ORP \approx 1\,deg\,\mu m^{-1}$), were formed (Figure 1 a,b). X-ray crystallographic studies performed for quickly cooled samples showed the structure typical for a lamellar crystal, with up to six harmonics of a main signal related to the layer thickness (being close to molecular length). The structure was distinctly different from those of crystal forms obtained by slow cooling (see the Supporting Information). For compounds **1** and **10**, a birefringent texture coexisting with some optically active domains was observed in quickly cooled samples. X-ray crystallographic measurements confirmed that for these materials a lamellar crystal coexisted with other crystal forms. Appa-

[*] Dr. J. Matraszek, N. Topnani, Prof. H. Takezoe, Prof. J. Mieczkowski, Dr. D. Pociecha, Prof. E. Gorecka
University of Warsaw, Department of Chemistry
ul. Żwirki i Wigury 101, 02-089 Warsaw (Poland)
Prof. N. Vaupotič
Department of Physics, Faculty of Natural Sciences and Mathematics
University of Maribor, Koroska 160, 2000 Maribor (Slovenia)
and
Jozef Stefan Institute, Jamova 39, 1000 Ljubljana (Slovenia)
Prof. H. Takezoe
Toyota Physical and Chemical Research Institute
41-1, Yokomichi, Nagakute, Aichi 480-1192 (Japan)

Supporting information for this article is available on the WWW under http://dx.doi.org/10.1002/anie.201510123.

  

***Table 1:*** Differential scanning calorimetry data for the materials studied. The transition temperatures are given in °C, the transition enthalpies (in parenthesis) in $J g^{-1}$. Bold rows indicate compounds that formed the B4 lamellar-type crystal upon fast cooling ($> 50\,°C\,min^{-1}$).

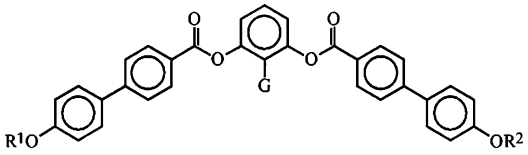


| Compound | G | $R^1$ | $R^2$ | Phase sequence | Gelation |
|---|---|---|---|---|---|
| **1** | **H** | **$C_5H_{11}$** | **$C_5H_{11}$** | **Cr1 112.5 (210.6) Cr2 178.5 (64.3) Iso** | + |
| **2** | **H** | **$C_8H_{17}$** | **$C_8H_{17}$** | **Cr1 146.4 (5.8) Cr2 159.3 (71.1) Iso** | + |
| **3** | **H** | **$C_{11}H_{23}$** | **$C_{11}H_{23}$** | **Cr 145.6 (44.2) Iso** | + |
| **4** | **H** | **$C_{12}H_{25}$** | **$C_{12}H_{25}$** | **Cr 143.6 (58.1) Iso** | **+ (precipitation)** |
| **5** | **H** | **$C_{16}H_{33}$** | **$C_{16}H_{33}$** | **Cr1 127.5 (11.3) Cr2 141.8 (66.2) Iso** | **+ (precipitation)** |
| **6** | H | $C_{16}H_{33}$ | (*R*) $CH(C_2H_5)C_5H_{11}$ | Cr 79.4 (45.8) Iso | – |
| **7** | H | (*R*) $CH(C_2H_5)C_5H_{11}$ | (*R*) $CH(C_2H_5)C_5H_{11}$ | Cr 74.2 (45.2) Iso | – |
| **8** | H | $C_{16}H_{33}$ | (*R*,*S*) $CH_2CH(C_{10}H_{21})C_{12}H_{25}$ | Cr 84.8 (36.4) Iso | – |
| **9** | H | (*R*,*S*) $CH_2CH(C_{10}H_{21})C_{12}H_{25}$ | (*R*,*S*) $CH_2CH(C_{10}H_{21})C_{12}H_{25}$ | Cr 44.7 (41.6) Iso | – |
| **10** | **$NO_2$** | **$C_8H_{17}$** | **$C_8H_{17}$** | **Cr 139.4 (57.5) Iso** | + |
| **11** | $NO_2$ | $C_{11}H_{23}$ | $C_{11}H_{23}$ | Cr 103.4 (23.3) B7 129.2 (31.1) Iso | – |

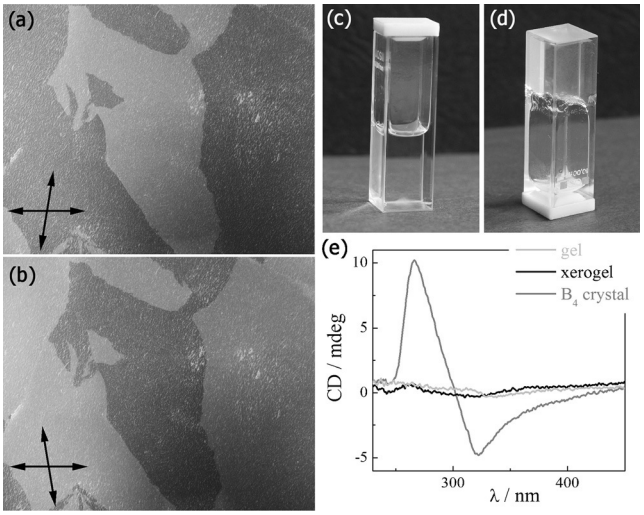


***Figure 1.*** a,b) Optical textures of compound **3** quickly cooled from the isotropic phase to room temperature, as observed with slightly decrossed polarizers. c) Sol and d) gel states for a solution of compound **2** in hexane. e) Circular dichroism spectra for samples of compound **2** in the gel, xerogel, and B4 crystal.

rently kinetic effects play an important role in the formation of the B4 phase for the studied compounds. For symmetrical homologues with branched terminal chains (compounds **7** and **9**) the isotropic phase was overcooled to room temperature. For asymmetric molecules with linear and branched terminal alkyl groups (compounds **6** and **8**), slow recrystallization was observed, and only optically inactive crystals were formed.

All the studied compounds with *n*-alkyl terminal chains showed gelation ability (at a concentration of ca. 1 mg/100 µl); the gelation occurred in just a few minutes in cyclohexane, and in more than an hour in toluene. The gels were nearly optically transparent (Figure 1 c,d). The sol–gel phase transition took place at approximately 50 °C in cyclohexane and at approximately 70 °C in toluene. For the longer homologues **4** and **5**, the gelation in toluene took place together with the precipitation of crystallites. For compounds with an $NO_2$ substituent at the central ring, gelation was observed only for a shorter homologue **10**, whereas for a longer homologue, **11**, microcrystals precipitated from solutions in both cyclohexane and toluene. None of the compounds with branched terminal chains showed gelation in any of the tested organic solvents; the compounds were well soluble in cyclohexane, hexane, and toluene. In more polar solvents, such as dichloroethane, no gelation was observed for any of the studied materials owing to their perfect solubility. The observations show that the ability to form a gel is mainly determined by the solubility of materials in a given solvent. Solubility decreases with elongation of the terminal *n*-alkyl chains, thus causing the precipitation of crystals, and increases with branching of the terminal alkyl chains.

X-ray crystallographic studies performed for the xerogel of **3** (after slow evaporation of the solvent) revealed its lamellar-type crystalline structure (see the Supporting Information). A significant broadening of the X-ray signals provided evidence that filaments forming gels consisted of stacks of a limited number of layers. The xerogel sample, which was heated to the isotropic phase and quickly cooled to form an optically active crystal, had a similar X-ray pattern with slightly sharper signals, thus suggesting that the crystal is built of aggregates with larger numbers of stacked layers. None of the xerogels were optically active. Moreover, for the gels and xerogels, no circular dichroism (CD) signal was observed at the molecular absorption band (ca. 300 nm), in contrast to the recrystallized samples, which showed a clear Cotton effect (Figure 1 e).

The studied materials, although weakly fluorescent in a solvent (quantum yield: ca. 0.1 for **6**) or the sol state, became highly fluorescent in the gel (an increase by two orders of magnitude as compared to the sol; see the Supporting Information) with redshifted emission (for compound **1** in cyclohexane, for the gel: $\lambda_{em} = 372$ nm, for the sol: $\lambda_{em} = 353$ nm). Thus, the studied compounds belong to the

relatively rare group of materials that become highly luminescent upon the formation of aggregates.[15] The redshift of the emission is evidence of favorable interactions between dipole transition moments of molecules within the crystal layers (J-aggregates),[15] whereas strongly enhanced fluorescence is likely a result of different molecular conformations in the sol and the gel. In aggregates, the intramolecular rotations of the molecules are strongly restricted, which blocks nonradiative pathways of energy dissipation and favors the light-emission pathway.

The morphology of both gels and crystals was studied by atomic force microscopy (AFM; Figure 2). The xerogels prepared from cyclohexane and toluene had similar morphology, thus suggesting that it is determined mainly by the crystal structure of the material rather than by interactions with the solvent. Interestingly, for gels of all studied compounds, apart from multilayer structures, monolayer and bilayer objects were also visible (Figure 2b; see also the Supporting Information); regions with saddle–splay deformed layers and well-developed helical ribbons were observed. The handedness of ribbons was correlated over at least a micron range. The

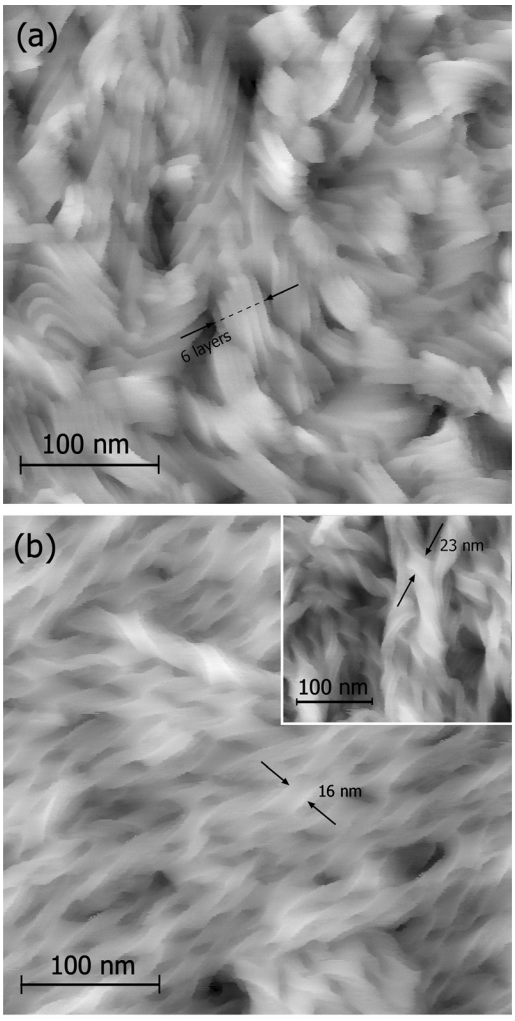


***Figure 2.*** AFM images of a) an optically active crystal (B4) of compound **5**, and b) the xerogel made from compound **2** (inset: xerogel of compound **3**).

geometrical parameters of helical filaments were found to depend on the molecular structure, that is, filaments were wider and helix pitches were longer for molecules with longer terminal chains (**1** ($n=5$): $w=7$–10 nm, $p=50$–60 nm; **2** ($n=8$): $w=15$–20 nm, $p=70$ nm; **3** ($n=11$): $w=20$–30 nm, $p=80$ nm; **4** ($n=12$): $w=30$–35 nm, $p=90$ nm). Since only the central part of the helical filament has an ideal saddle–splay curvature that minimizes the elastic energy,[16] and surfaces of the filament have slightly higher energies, twisting is less favorable for thicker slabs. Therefore, longer helix pitches are expected for molecules with longer tails, as experimentally observed. The dependence of the width of the filament on the molecular length can be explained by the tendency for spontaneous splay (in the orientation of the molecular tips), characteristic for bent-core systems, which leads to either the undulation of smectic layers or the breakdown of layers into columns.[17] The increase in the filament width, $w$, with increasing length of the terminal chains suggests that the elastic constant for splay deformation increases with the length of the terminal chains. Thus, splay deformation appears to be driven by entropic effects (longer tails obtain more space for fluctuations) rather than by steric effects (splay as a result of the greater thickness of the molecular cores as compared to the ends).[18]

If the xerogel was heated to the isotropic phase and subsequently quickly cooled, optically active crystals were grown. For such samples, twisted stacks of few layers (ca. 5–6) were observed in AFM images (Figure 2a), with a layer periodicity that agreed well with that determined by the X-ray diffraction studies. For recrystallized samples, usually no well-defined structure of filaments was found, but some areas with saddle–splay deformations could be clearly distinguished. Thus, it is likely that the optical activity is caused by the internal layer structure (layer optical activity, LOA)[19] rather than by the helicity of the ribbons. The LOA is a result of a strongly inhomogeneous distribution of electron density inside the layers. Moreover, it is known that the optical activity is negligible for nematic or smectic phases with short helical structures, such as ferroelectric chiral smectic phases,[20] if the wavelength of light is much longer than the helix pitch ($\lambda > 5p$), which is the case for the filaments in this study. It can be expected that the magnitude of LOA is related to the number of stacked layers. Calculations for slabs made of a limited number of layers (see the Supporting Information), according to the model proposed by Hough and Clark[19] to explain the optical activity of the $SmC_SP_F$ and $SmC_AP_A$ smectic phases, show that the ORP quickly increases as the number of layers increases and saturates for slabs with few layers (Figure 3). By inserting typical values for the refractive index and layer thickness, it was found that the saturated value of ORP is of the order of degrees per micron, comparable to the value measured in bulk samples of the materials. For gels (and xerogels), this value is likely to be considerably lower, since they are built up of thinner slabs.

It was expected that the filament nanostructures, owing to their high surface-to-volume ratio, can enhance the dissociation of excitons and promote the conduction of holes in photovoltaic devices.[21] The photovoltaic properties of xerogels composed of mixtures of compound **1** or **5** with

  

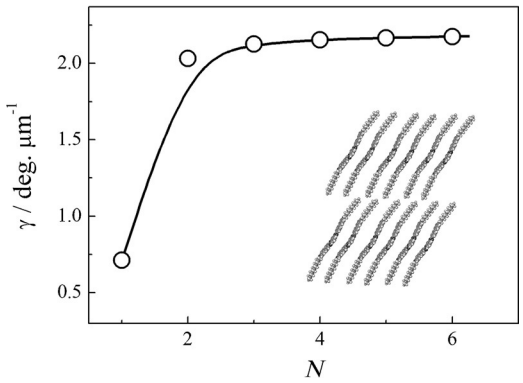


***Figure 3.*** Calculated optical rotatory power ($\gamma$) as a function of the number of layers ($N$) in the slab. The arrangement of molecules in the layer is also shown; the molecules form a lamellar crystal with a monoclinic structure.

approximately 5 wt% of a fullerene derivative (see the Supporting Information for the molecular structure) were tested; the fullerene unit is well-known for its electron-accepting properties.[22] The gels were prepared in toluene, and the solvent was evaporated. The obtained xerogels were examined by X-ray diffraction and AFM. The lack of X-ray signals other than those related to the crystal structure of bent-core compounds indicated that the fullerene derivative was encapsulated in its liquid (or glassy) state between the filaments made of bent-core molecules. Upon irradiation with UV light, the xerogels showed strongly quenched fluorescence (see the Supporting Information), thus suggesting the deactivation of the excited state by a nonradiative process,[23] possibly by electron transfer from the bent-core molecules to fullerene molecules, resulting in the formation of an intermolecular charge-separated state. Unfortunately, no photocurrent was registered, showing that the conducting properties of the ribbons are very weak, either because of their monolayer structure or because of the presence of a large number of defects.

To summarize, although the B4 lamellar crystal structure is essentially the same in gel and bulk samples, the morphology is different. In bulk samples, strongly distorted stacks of a few (5–6) molecular layers are formed, whereas in the gel a considerable number of objects made of monolayers and bilayers were found. The filaments that are formed in gels have the width and pitch dependent on the molecular structure. Although in both the bulk and the gel samples the chiral symmetry is broken at microscale, their optical activity is different, as it is related to the arrangement of molecules and the number of layers in stacks, rather than to the helicity of the filaments; the optical activity increases with an increasing number of layers and saturates for 3–4 layers in stacks. The large number of monolayers and bilayers are likely to be responsible for the lack of optical activity and a CD signal in gels (and xerogels). The optical activity appears for the bulk sample owing to the greater thickness of slabs.


## Acknowledgements

The research was financed by project NCN DEC-2012/07/B/ST5/02448; the organic synthesis was financed by project NCN UMO-2012/05/B/ST5/00725. N.V. acknowledges the support of the research program P1-0055 of the Slovenian Research Agency.

**Keywords:** bent-core molecules · chiral symmetry breaking · gels · helical nanofilaments · liquid crystals

**How to cite:** *Angew. Chem. Int. Ed.* **2016**, *55*, 3468–3472
*Angew. Chem.* **2016**, *128*, 3529–3533



[1] P. Terech, R. G. Weiss, *Chem. Rev.* **1997**, *97*, 3133.
[2] J. Puigmartí-Luis, A. P. del Pino, V. Laukhin, L. N. Feldborg, C. Rovira, E. Laukhina, D. Amabilino, *J. Mater. Chem.* **2010**, *20*, 466.
[3] a) N. M. Sangeetha, U. Maitra, *Chem. Soc. Rev.* **2005**, *34*, 821; b) T. Kato, N. Mizoshita, M. Moriyama, T. Kitamura, *Top. Curr. Chem.* **2005**, *256*, 219.
[4] a) A. Brizard, R. Oda, I. Huc, *Top. Curr. Chem.* **2005**, *256*, 167; b) J. H. Van Esch, B. L. Feringa, *Angew. Chem. Int. Ed.* **2000**, *39*, 2263; *Angew. Chem.* **2000**, *112*, 2351; c) K. Murata, M. Aoki, T. Suzuki, T. Harada, H. Kawabata, T. Komori, F. Ohseto, K. Ueda, S. Shinkai, *J. Am. Chem. Soc.* **1994**, *116*, 6664.
[5] S.-C. Lin, R.-M. Ho, C.-Y. Chang, C.-S. Hsu, *Chem. Eur. J.* **2012**, *18*, 9091.
[6] X. Ran, P. Zhang, S. Qu, H. Wang, B. Bai, H. Liu, C. Zhao, M. Li, *Langmuir* **2011**, *27*, 3945.
[7] a) M. Cano, A. Sánchez-Ferrer, J. L. Serrano, N. Gimeno, M. B. Ros, *Angew. Chem. Int. Ed.* **2014**, *53*, 13449; *Angew. Chem.* **2014**, *126*, 13667; b) S.-C. Lin, T.-F. Lin, R.-M. Ho, C.-Y. Chang, C.-S. Hsu, *Adv. Funct. Mater.* **2008**, *18*, 3386.
[8] D. Chen, C. Zhu, H. Wang, J. E. Maclennan, M. A. Glaser, E. Korblova, D. M. Walba, J. A. Rego, E. A. Soto-Bustamante, N. A. Clark, *Soft Matter* **2013**, *9*, 462.
[9] A. Zep, M. Salamonczyk, N. Vaupotič, D. Pociecha, E. Gorecka, *Chem. Commun.* **2013**, *49*, 3119.
[10] a) Y. Takanishi, G. J. Shin, J. C. Jung, S.-W. Choi, K. Ishikawa, J. Watanabe, H. Takezoe, P. Toledano, *J. Mater. Chem.* **2005**, *15*, 4020; b) C. Zhu, D. Chen, Y. Shen, C. D. Jones, M. A. Glaser, J. E. Maclennan, N. A. Clark, *Phys. Rev. E* **2010**, *81*, 011704.
[11] K. Fodor-Csorba, A. Vajda, A. Jákli, C. Slugovc, G. Trimmel, D. Demus, E. Gács-Baitz, S. Hollye, G. Galli, *J. Mater. Chem.* **2004**, *14*, 2499.
[12] S. Chakraborty, J. T. Gleeson, A. Jakli, S. Sprunt, *Soft Matter* **2013**, *9*, 1817.
[13] S. Pelzl, G. Diele, A. Jakli, C. Lischka, I. Wirth, W. Weissflog, *Liq. Cryst.* **1999**, *26*, 135.
[14] E. Gorecka, N. Vaupotič, D. Pociecha, *Chem. Mater.* **2007**, *19*, 3027.
[15] a) F. Würthner, T. E. Kaiser, C. R. Saha-Möller, *Angew. Chem. Int. Ed.* **2011**, *50*, 3376; *Angew. Chem.* **2011**, *123*, 3436; b) Y. Hong, J. W. Y. Lam, B. Z. Tang, *Chem. Soc. Rev.* **2011**, *40*, 5361.
[16] a) L. E. Hough, H. T. Jung, D. Krüerke, M. S. Heberling, M. Nakata, C. D. Jones, D. Chen, D. R. Link, J. Zasadzinski, G. Heppke, J. P. Rabe, W. Stocker, E. Körblova, D. M. Walba, M. A. Glaser, N. A. Clark, *Science* **2009**, *325*, 456; b) R. D. Kamien, *Rev. Mod. Phys.* **2002**, *74*, 953.
[17] N. Vaupotič, M. Čopič, E. Gorecka, D. Pociecha, *Phys. Rev. Lett.* **2007**, *98*, 247802.
[18] C. Bailey, A. Jákli, *Phys. Rev. Lett.* **2007**, *99*, 207801.
[19] L. E. Hough, N. A. Clark, *Phys. Rev. Lett.* **2005**, *95*, 107802.

[20] T. Akizuki, K. Miyachi, Y. Takanishi, K. Ishikawa, H. Takezoe, A. Fukuda, *Jpn. J. Appl. Phys.* **1999**, *38*, 4832.
[21] a) K. Yoshino, X. H. Yin, K. Muro, S. Kiyomatus, S. Morita, A. A. Zakhidov, T. Noguchi, T. Ohnishi, *Jpn. J. Appl. Phys.* **1993**, *32*, L357; b) R. A. Callahan, D. C. Coffey, D. Chen, N. A. Clark, G. Rumbles, D. M. Walba, *ACS Appl. Mater. Interfaces* **2014**, *6*, 4823.
[22] R. C. Haddon, L. E. Brus, K. Raghavachari, *Chem. Phys. Lett.* **1986**, *125*, 459.
[23] G. Bottari, G. de la Torre, D. M. Guldi, T. Torres, *Chem. Rev.* **2010**, *110*, 6768.

Received: October 30, 2015
Revised: December 9, 2015
Published online: February 2, 2016

  